SAND2019-7034C

Effect of Mineral Orientation on Roughness and Toughness of Mode I Fractures

Liyang Jiang
Department of Physics and Astronomy, Purdue University, West Lafayette, IN,USA
Hongkyu Yoon
Geomechanics Department, Sandia National Laboratories, Albuquerque, NM,USA
Antonio Bobet
Lyles School of Civil Engineering, Purdue University, West Lafayette, IN,USA
Laura J. Pyrak-Nolte
Department of Physics and Astronomy, Purdue University, West Lafayette, IN,USA
Lyles School of Civil Engineering, Purdue University, West Lafayette, IN,USA
Department of Earth and Atmospheric Sciences, Purdue University, West Lafayette, IN,USA

ABSTRACT: Anisotropy in the mechanical properties of rock is often attributed to layering or mineral texture. Here, results from a study on mode I fracturing are presented that examine the effect of layering and mineral orientation fracture toughness and roughness. Additively manufactured gypsum rock was created through 3D printing with bassanite/gypsum. The 3D printing process enabled control of the orientation of the mineral texture within the printed layers. Three-point bending (3PB) experiments were performed on the 3D printed rock with a central notch. Unlike cast gypsum, the 3D-printed gypsum exhibited ductile post-peak behavior in all cases. The experiments also showed that the mode I fracture toughness and surface roughness of the induced fracture depended on both the orientation of the bedding relative to the load and the orientation of the mineral texture relative to the layering. This study found that mineral texture orientation, chemical bond strength and layer orientation play dominant roles in the formation of mode I fractures. The uniqueness of the induced fracture roughness is a potential method for the assessment of bonding strengths in rock.

1. INTRODUCTION

Understanding the mechanical behavior of layered rock is vital in hydraulic fracturing for the exploitation of shale gas and oil reservoirs. The complex response of shale is, in part, caused by anisotropy from layering within the rock. Anisotropy is often a common characteristic of rock because of natural geological processes, which deposit sediments sequentially in layers or metamorphic processes that align mineral grains. The orientation of layers/bedding relative to in-situ and induced stresses can significantly affect rock strength and deformation. Layers are often natural planes of weakness that can debond when stresses attain a failure condition. Previous studies have shown that rock strength depends on the direction of fracture propagation relative to layering (Gao et al., 2017, Chandler et al., 2016, Na et al., 2017). In those studies, samples are often referred to as arrester (Figure 1 H and Halt), divider, and short traverse (Figure 1 V and Valt). A number of studies on shale have found that fracture toughness is greatest for divider samples (e.g. Gao et al., 2017), while others have observed that the short traverse samples can exhibit both the largest and smallest values of fracture toughness (Chandler et al., 2016, Na et al., 2017). Variation in behavior relative to layering is often attributed to heterogeneity, clays, fluids, etc. A difficulty in linking layer orientation to fracture toughness is the variability of rock. Often, even samples taken from the same outcrop or rock block exhibit different peak strengths. Laboratory samples with repeatable mineral fabric and structural features are required to better understand the role of layering on peak failure load or fracture toughness in layered material. It is difficult to achieve uniform properties across cohorts of samples when working with natural rock.

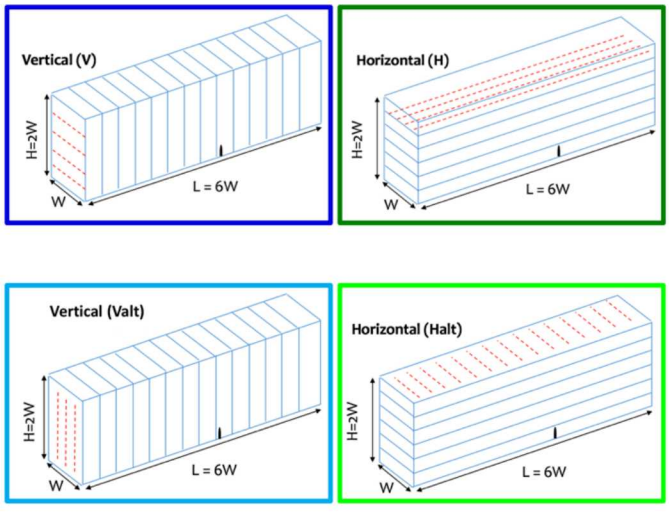

Fig. 1. 3D printed samples showing the orientation of the bassanite layers (blue lines), gypsum texture (red lines).

Sandia National Laboratories is a multimission laboratory managed and operated by National Technology & Engineering Solutions of Sandia, LLC, a wholly owned subsidiary of Honeywell International Inc., for the U.S. Department of Energy's National Nuclear Security Administration under contract DE-NA0003525.

To overcome this challenge, we fabricated a layered synthetic rock using 3D printing to test the effect of layer orientation on mode I fracture toughness. We observed that it is insufficient to predict fracture resistance from consideration of layer orientation alone, and that the orientation of mineral texture, within the layers, also influences fracture toughness and roughness.

2. SAMPLE PREPARATION

Analog rock samples were created using a 3D printing process (ProJet CJP 360 printer). Layers of calcium sulfate hemi-hydrate (0.1 *mm* thick bassanite powders) were bonded with a proprietary water-based binder (ProJet X60 VisiJet PXL), resulting in a gypsum (calcium sulfate hemi-hydrate) reaction product. The gypsum mineral growth direction is influenced by the direction of the binder spreading. When one layer of bassanite is deposited on a previous layer, the gypsum crystals form a bond between bassanite layers. Texture arises because stronger bonds are formed amongst gypsum crystals than between gypsum crystals and bassanite powder (Figure 2 *left*).

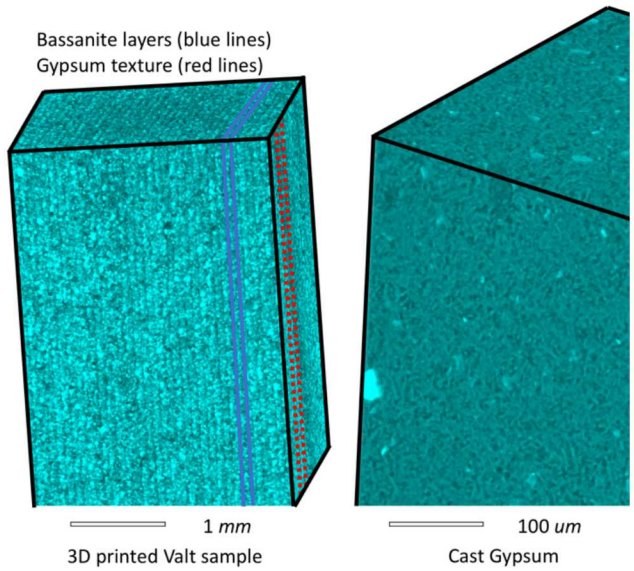

Fig. 2. 3D Xray CT computed tomography of one part of a 3D printed gypsum sample showing the layering and the in-layer oriented mineral growth of sample Valt (*left*), and one part of a cast gypsum sample with no preferred mineral orientation (*right*).

Samples with different orientations of bassanite layers relative to gypsum texture were 3D printed to examine the effect of texture direction relative to layer direction on mode I crack growth. Three-point bending (3PB) experiments were conducted on printed specimens (25.4 x 76.2 x 12.7 *mm*) with a 5.08 *mm* long 1.27 *mm* wide central notch, to induce a mode I crack.

Non-layered reference samples (Figure 2 *right*) with no preferred mineral orientation were created by casting gypsum in a mold. A silicon rubber mold was created from a solid resin sample (3D printed on a FormLabs 2) with the same dimensions as the 3D printed samples. The mold was filled with mixed gypsum and water and then vibrated to minimize the amount of trapped air. The cast gypsum samples were then cured in an oven at 40 *°C* for 4 days.

3. EXPERIMENTAL SETUP

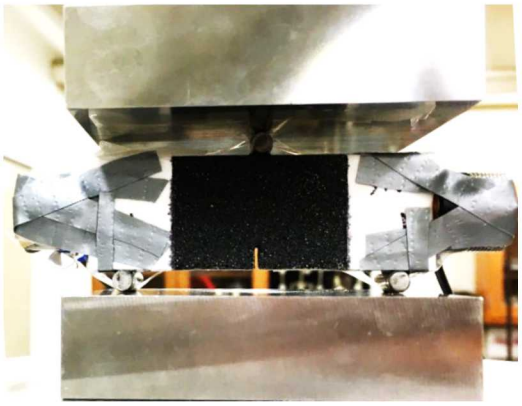

Fig. 3. Experimental setup: 3PB sample with top and bottom rods, acoustic transducers attached, and a speckled region on front surface for DIC.

A three-point bending (3PB) method (Figures 3 and 4) was used to induce a tensile fracture (Mode I) in the 3D printed and cast samples. Three rods were placed on the sample: one centered at the top, and the other two at the bottom (Figure 3). On each side of the sample, ultrasonic transducers were attached to measure either transmitted compressional (P) or shear (S) seismic signals. Dark speckle spray paint was applied at the center of the front surface to achieve a random black-white-grey speckled region (38 *mm* in height by 25 *mm* in width) for Digital Image Correlation (DIC), which is a useful technique to measure surface displacements during loading.

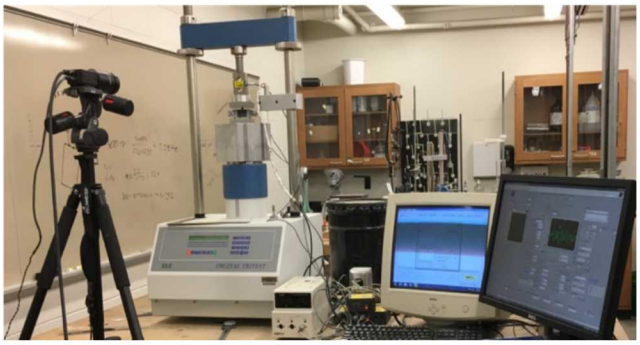

Fig. 4. Loading frame and camera setup.

DIC is a particle tracking method that can be used to determine displacements on the surface of a sample. A Grasshopper 3 CMOS camera (12.3 *MP*, 3.54 *um* resolution) from the FLIR company and a Tamron 50 *mm* lens (f/1.8 aperture) were used to acquire images of the speckled region during loading (Figure 4). For additional information on the technique and analysis methods, the reader is referred to Scriven et al., (2007), Pan et al., (2009) and Hedayat et al. (2014).

Load was applied to a sample using an ELE International Soil Testing load frame with a 2000 *lbs* (8896 *N*) capacity S-shaped load cell (Figure 4). The test was conducted using a loading rate of 0.03 *mm/min*. Load and displacement (from a LVDT) data were recorded at a 5 *Hz* recording rate.

Olympus Panametrics piezoelectric contact transducers (V-103 and V-153) were used to send and receive ultrasonic (central frequency of 1 *MHz*) signals (P or S waves) as shown in Figure 3. Shear wave measurements were made with the source and receiver transducers polarized perpendicular to the long axis of the notch (i.e. in the direction of fracture propagation). All measurements were made at normal incidence to the fracture plane. The transducers were coupled to the sample with oven baked honey (8.75 % weight loss after oven-baked at 90 °*C*). An Olympus 5077PR pulse generator, set at 400 *V* excitation with a 1 *MHz* repetition frequency was used to excite the piezoelectric transducers. The ultrasonic waves were digitized using a National Instruments USB-5133 digitizer and stored on a computer for analysis. A sampling rate of 100 MSamples/sec. was used to get a bin size of 0.01 microseconds.

4. RESULTS: FRACTURE FAILURE

3PB is often used to determine mode I fracture toughness because minimal alignment is required between the notch and the load application, which makes the test attractive compared to other tests. The sample is placed on two pins and the load is applied through a pin centered on the top of the sample (Whittaker et al., 1992).

The fracture toughness of the material can be obtained from solutions of the for $K_{Ic} = \frac{PS}{BW^{3/2}} f(\frac{a}{W})$, where P is the maximum (or peak) applied load, B is the thickness of the specimen, S is the distance between the bottom two rods, 2a is the crack length, and W is the width of the specimen (Whittaker et al., 1992). In 3PB tests, a fatigue crack may be created at the tip of the notch by cyclic loading, prior to testing (ASTM Standard C1421-18, ASTM Standard E1820-18a). In our approach, a pre-existing notch is 3D printed instead of being created by loading. By printing the notch, the repeatability of the tests is improved. However, the fracture toughness will be over-estimated because the printed notch does not have a sharp tip. In the following, we use fracture toughness and peak load interchangeably, even though it may not be entirely correct, given the blunt notch in the experiments. The discussion, however, is independent of this consideration.

Figure 5 shows the load-displacement data for the four 3D printed geometries shown in Figure 1, and for a cast gypsum sample. The short traverse samples (V and Valt) had similar peak loads and were the lowest of all the tests. The 3D printed samples exhibited relatively ductile post-peak behavior (Figure 5), unlike the cast gypsum, where failure was abrupt once the peak load was reached. Cast gypsum samples were stiffer than the 3D printed samples.

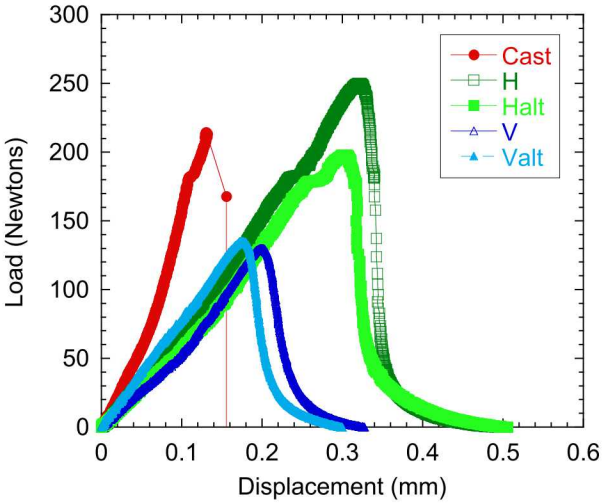

Fig. 5. Load displacement curves of cast gypsum and 3D printed samples.

The fracture toughness ratio (fracture toughness normalized with that of the H sample) is given in Figure 6 for all the tests. Results are shown for three cohorts, with each cohort containing a cast gypsum sample and the four 3D printed geometries. Mode I fracture toughness is observed to depend on both the orientation of the bedding relative to the load and on the orientation of the mineral texture relative to the layering (Figure 6). The largest values for mode I fracture toughness were found when the mineral texture orientation and layering were perpendicular to the failure plane (samples H in Figure 1), while the smallest values were observed when both the layering and mineral orientations were parallel to the failure plane (samples V and Valt in Figure 1).

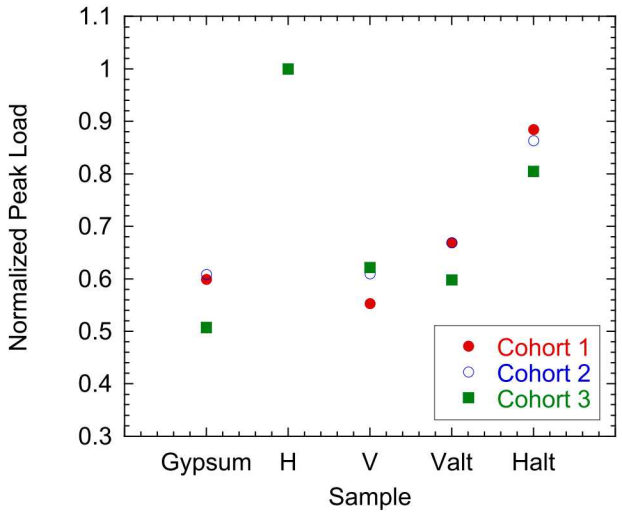

Fig. 6. Fracture toughness normalized with respect of the fracture toughness of sample H, for three test cohorts (repeatability tests).

5. RESULTS: FRACTURE ROUGHNESS

Laser profilometry was performed to quantify the asperity height and roughness of the induced tensile crack surfaces, with a 0.1 *mm* spatial resolution. The surface geometry of the cast gypsum is shown in Figure 7, and is used as the base case for comparisons with the 3D printed samples. Surface roughness measurements were used to describe the texture of the mode I fracture surface and to obtain the micro-slope angles (i.e. local slope) of the asperities on the surface. As shown in Figure 7, the surface of the mode I fracture in cast gypsum was relatively smooth (only varying between +/- 15°) and the micro-slope angle distribution was isotropic (parallel and perpendicular to fracturing).

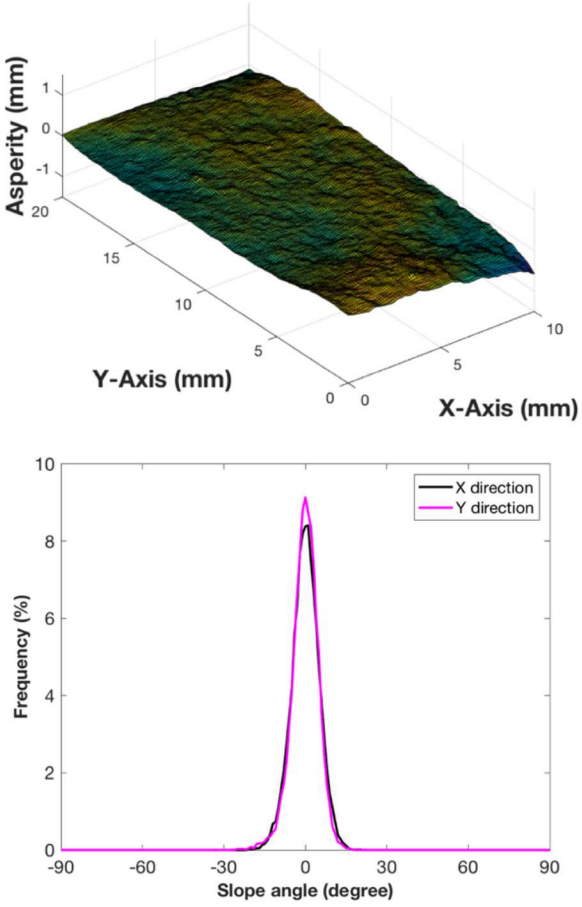

Fig. 7. Asperity height and micro-slope angle distribution of mode I fracture from a cast gypsum sample.

To compare the micro-slope frequency distributions, the half width of the distribution curve was measured between those points with a frequency value equal to half the maximum frequency. This is known as the half width at half maximum (HWHM). Figure 8 shows average values of HWHM of the micro-slope angle distributions for the cast gypsum and the 3D printed samples. The surface roughness of the induced fractures depended on the orientation of the load relative to the layering and mineral direction. For the 3D printed samples, surface roughness was direction-dependent. We hypothesize that the relative strength of the bassanite-bassanite, bassanite-gypsum, and gypsum-gypsum bonds controlled the HWHM of the micro-slope distribution (Figure 8). The smoothest cracks were formed when the mineral direction and layering were both parallel to the failure plane (Figure 1 sample V and Valt). For samples with only mineral direction parallel to the failure plane (Figure 1 sample Halt), the micro-slope angle distribution was anisotropic. The HWHM of the micro-slope frequency distribution of sample Halt (Figure 1) differed more in the directions parallel and perpendicular to fracture propagation compared to sample H (Figure 1). We also observed that the high values of toughness (Figures 6) correlated with rougher surfaces (Figures 8).

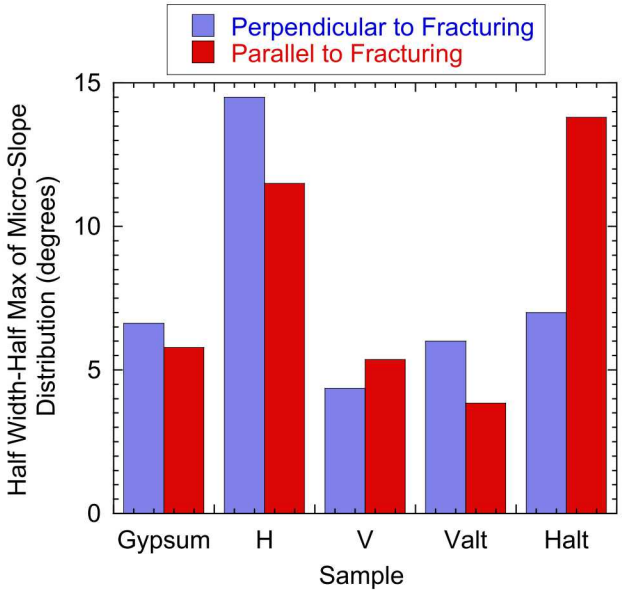

Fig. 8. Average of micro-slope frequency distribution HWHM for cast gypsum and 3D printed samples (H, Halt, V, and Valt), parallel and perpendicular to the direction of fracture propagation.

6. SUMMARY

3D printed gypsum samples exhibit less variability in behavior than natural rock samples, which makes the technique very attractive to isolate, and investigate the effects of a particular characteristic of the rock, one at a time. Peak failure loads among manufactured cohorts varied from 10 to 12% in magnitude, and the trends were always consistent in terms of preparation (layering and texture) and strength. Interestingly, 3D printing produces an anisotropic material. Anisotropy arises from two sources: (1) layering; and (2) direction of mineral texture. Failure load on 3PB tests is the smallest when the layering is parallel to the fracture plane, and is the largest when the mineral texture direction is perpendicular to the fracture plane. Whether the surface roughness of the induced tensile crack is isotropic or anisotropic depends on both the layering and mineral texture directions relative to the direction of fracture propagation.

The paper presents limited results of an ongoing project and, while not intended to provide a comprehensive picture of the interrelationship that exists between layering, texture, fracture load and surface characteristics, it does point to the key effects of layering and texture on fracture toughness and roughness, and to the advantages and disadvantages of using additive manufacturing to simulate and study the complexities of natural rock.

7. ACKNOWLEDGMENTS

Sandia National Laboratories is a multi-mission laboratory managed and operated by National Technology & Engineering Solutions of Sandia, LLC, a wholly owned subsidiary of Honeywell International, Inc., for the U.S. Department of Energy's National Nuclear Security Administration under contract DE-NA0003525. This work is supported by the Laboratory Directed Research and Development program at Sandia National Laboratories. This paper describes objective technical results and analysis. Any subjective views or opinions that might be expressed in the paper do not necessarily represent the views of the U.S. Department of Energy or the United States Government.

REFERENCES

1. ASTM C1421-18 Standard Test Methods for Determination of Fracture Toughness of Advanced Ceramics at Ambient Temperature, ASTM International, West Conshohocken, PA, 2018, https://doi.org/10.1520/C1421-18
2. ASTM E1820-18a Standard Test Method for Measurement of Fracture Toughness, ASTM International, West Conshohocken, PA, 2018, https://doi.org/10.1520/E1820-18A
3. Chandler, M.R., Meredith, P.G., Brantut, N., Crawford, B.R. Fracture toughness anisotropy in shale (2016) *Journal of Geophysical Research: Solid Earth*, 121 (3), pp. 1706-1729
4. Gao, Y., Liu, Z., Zeng, Q., Wang, T., Zhuang, Z., Hwang, K.-C. Theoretical and numerical prediction of crack path in the material with anisotropic fracture toughness (2017) *Engineering Fracture Mechanics*, 180, pp. 330-347.
5. Hedayat, A., Pyrak-Nolte, L. and Bobet, A. (2014). Detection and Quantification of Slip along Non-uniform Frictional Discontinuities using Digital Image Correlation. *ASTM Geotechnical Testing Journal*. DOI: 10.1520/GTJ2013.
6. Na, S., Sun, W., Ingraham, M. D., & Yoon, H. (2017). Effects of spatial heterogeneity and material anisotropy on the fracture pattern and macroscopic effective toughness of Mancos Shale in Brazilian tests. *Journal of Geophysical Research: Solid Earth*, 122(8), 6202-6230.
7. Pan, B., K. Qian, H. Xie, and A. Asundi. 2009, Two-dimensional digital image correlation for in-plane displacement and strain measurement: A review, *Meas. Sci. Technol*, 20, 062001, doi:10.1088/0957-0233/20/6/062001.
8. Scrivens, W. A., Luo, Y., Sutton, M. A., Collette, S. A., Myrick, M. L., Miney, P., & Li, X. 2007. Development of patterns for digital image correlation measurements at reduced length scales. *Experimental Mechanics*, 47(1), 63-77
9. Whittaker, B.N., Singh, R.N., Sun, G., 1992. *Rock Fracture Mechanics—Principles, Design and Applications*. Elsevier, Amsterdam.